Jurnal Teknologi, 41(F) Keluaran Khas. Dis. 2004: 101–112

MEASURING THE BINDING OF AN ANTIMICROBIAL PEPTIDE WITH LPS BY FLUORESCENCE CORRELATION SPECTROSCOPY

LANLAN YU[1], BOW HO[2], JEAK LING DING[3] & THORSTEN WOHLAND[4*]

Abstract. Antimicrobial peptides are an important defense weapon of many organisms, which attack the membrane of bacteria, leading to inhibition of bacterial growth and finally, bacterial death. Despite their ancient origin, it is difficult for bacteria to develop resistance against these peptides. This makes antimicrobial peptides a promising candidate for new drugs against microbial diseases. The target of these peptides is lipopolysaccharides (LPS), which are the major component of the outer membrane of Gram-negative bacteria. Known peptide structures and computational models show an amphipathic cationic pattern BHPHB (B: basic; H: hydrophobic; P: polar residue, respectively), which is the possible binding site of antimicrobial peptides to LPS. A cyclic amphipathic cationic 19-residue peptide (V4) with one disulfide bond has been designed (Frecer et al., unpublished data), which has potential antimicrobial activity. Circular dichroism measurements showed that V4 has a β-sheet structure. The interaction of a fluorophore labeled-V4 with LPS has been investigated by fluorescence correlation spectroscopy (FCS). The study demonstrated that V4 can specifically bind LPS, in contrast to zwitterionic phosphatidylcholine (PC) of eukaryotic cells. FCS makes it possible to study the binding between peptide and LPS at low concentration in vitro. The dissociation constant of the peptide and LPS was obtained using this technique.

Keywords: antimicrobial peptides, LPS, peptide-lipid interaction, fluorescence correlation spectroscopy

1.0 INTRODUCTION

Antimicrobial peptides (AMPs) play a vital function in biological processes of host defense systems and innate immunity. Their ability to rapidly defend against infection by a broad range of bacteria confers significant antibiotic properties on these AMPs against invading microbes. AMPs are widely found in insects, amphibians, and mammals, including humans [1-4]. More than 500 AMPs have been discovered. However, many of these peptides have membrane-lytic ability against eucaryotic cells or prokaryotic cells, or both [5]. Many characteristics of AMPs have been investigated and more derivatives based on the natural peptides, whose antimicrobial activity is

[1&4] Department of Chemistry, Faculty of Science, National University of Singapore, 117543, Singapore.
[2] Department of Microbiology, Faculty of Science, National University of Singapore, 117543, Singapore.
[3] Department of Biological Science, Faculty of Science, National University of Singapore, 117543, Singapore.
* Corresponding author: Email: chmwt@nus.edu.sg

increased, have been designed. These AMPs mainly attack bacterial membrane and form pores leading to membrane permeabilization and finally, bacterial death. Great efforts have been exerted on unraveling the mechanism by which, the AMPs associate specifically with bacterial membrane, and the optimization of the orientation when binding to membranes, to induce pores [6]. The maintenance of antimicrobial activity of D-amino acid enantiomers and L-amino acid enantiomers indicates that there is no stereospecific interaction with antimicrobial activity [7].

Previous studies have shown that most natural AMPs are net positively charged, and also harbor some hydrophobic amino acid residues, in spite of considerable variation in primary structure and length [6]. The AMPs are cationic under physiological conditions and amphipathic structures are formed, when they approach and bind to bacterial membranes. Electrostatic and hydrophobic interactions drive the above process. The AMPs can be divided into two main structural classes. An α-helix conformation is adopted by most AMPs, when they bind to membranes. These linear peptides have no structure in solution, but when they are in a hydrophobic environment such as a membrane, in lipid or detergent, an α-helix conformation is induced. Examples of this class include insect cecropins [8], frog magainins [4], and human cathelicidins [9]. The second structural class comprises of peptides with β-sheet structures, which usually possess disulfide bonds, which stabilize the conformation. Mammalian defensins [10] and protegrins [11] belong to this class. Two main mechanisms are proposed to explain how α-helical antimicrobial peptides lyse the bacterial membranes. In the "barrel-stave" model [12], the amphipathic α-helices insert into the hydrophobic core of the membrane and form transmembrane pores with the hydrophobic part of the peptide "attaching" to the lipid, and the hydrophilic part of peptides pointing inward, forming an aqueous pore [5]. In this case, the mechanism of interaction between the AMPs and bacterial membranes is mainly dependent on hydrophobic interactions, and net charge is less important. In the "carpet" mechanism [13, 14], AMPs bind to the head group of membrane lipids and initially, cover the surface of the membrane. When the local concentration of AMPs reaches a threshold value, they disrupt the membrane, and make it permeable. This process is initially driven by electrostatic interactions, and therefore, net positively charged peptides are required. The main target of AMPs is lipopolysaccharides (LPS), which are the major component of the outer membrane of Gram-negative bacteria. The release of LPS within the host can cause severe bacterial sepsis [15]. LPS, which is negatively charged is composed of three parts: O-antigen, polysaccharide, and lipid A. Lipid A is the bioactive component of LPS, which is responsible for most of the endotoxic effects. It has been shown that lipid A is the main interacting partner with AMPs. Known peptide structures and computational models show an amphipathic cationic pattern BHPHB (B: basic; H: hydrophobic; P: polar residue, respectively), which is the possible binding site of AMPs to LPS. Therefore, a cyclic amphipathic cationic 19-residue peptide named V4, with one

disulfide bond has been designed [15]. It has potential antimicrobial activity. The sequence of V4 is CVKVQVKVGSGVKVQVKVC with cyclization by a disulfide bond at two cysteines (C). Four lysines (K) residues provide high net positive charge and eight valines (V) residues make this peptide highly hydrophobic. Circular dichroism (CD) measurements showed that the peptide has a β-sheet structure in water [15].

The interaction between AMPs and bacterial membranes has been investigated by a variety of techniques. CD spectra offers information about the secondary structure of peptides before, and after binding to membrane, and has became a popular technique in studying AMPs. Several organic solvents and detergents are used to mimic the hydrophobic membrane environment, as well as a variety of lipids [16]. Nuclear magnetic resonance (NMR), especially solid-state NMR, can also give information about the conformation a peptide adopts when binding to lipids. Cecropin A has been reported to adopt a helix-turn-helix conformation in the aqueous hexafluoroisopropanol using NMR [17]. Other methods such as attenuated total reflection Fourier transform infrared spectroscopy (ATR-FTIR), fluorescence spectroscopy, reversed phase-high performance liquid chromatography, surface plasmon resonance, Raman spectroscopy, and oriented circular dichroism (OCD) spectroscopy (reviews in [16, 17]) are also been applied to study the binding interaction. Fluorescence correlation spectroscopy (FCS) is a single molecule sensitive technique, which can measure biomolecular interactions in concentration ranges between 0.1 nM up to several μM. FCS can measure in extremely small volumes (~μ L) and gives access to diffusion coefficients, and concentrations with very high resolutions. This is achieved by using a diffraction limited confocal volume. In this study, we labeled the V4 peptide with tetramethylrhodamine (TMR) and investigated the interaction of V4 peptide and LPS using FCS, which provides new information about artificial antimicrobial peptide.

2.0 MATERIALS AND METHOD

2.1 Materials

Rhodamine 6G chloride and TMR were purchased from Molecular Probes (ITS Science and Medical Pte Ltd, Singapore). LPS from Escherichia coli strain 0111:B4, Lipid A from Escherichia coli strain F583, and PBS buffer were purchased from Sigma-Aldrich. DMSO was purchased from Mallinckrodt Baker, Inc. PC was purchased from Avanti polar lipids, Inc. V4-TMR at 75% purity was synthesized by Genemed Synthesis, Inc, USA. The purity was checked by reversed-phase HPLC and MS. The N-terminus was labeled with TMR. The stock solution of peptide was prepared as a 2mM solution in DMSO and stored at –20°C in small aliquots until further use.

2.2 FCS Instrumentation

FCS experiments were performed using a Zeiss microscope. The laser beam was focused on the samples using a water immersion objective (C-Apochromat, 63×, NA 1.2). A dichroic filter (570DRLP) and an emitter (595AF30) were used to separate the excitation light from the emission fluorescence. The samples were excited with the 530nm line of laser. The power used in the experiments was 100 μW. A pinhole in the image plane was placed to block the fluorescence that was not from the focal region. The emitted fluorescence was detected by an avalanche photo diode (APD) (PerkinElmer) detector and then the signals were sent to a digital correlator (www.correlator.com) to be autocorrelated.

2.3 FCS Data Evaluation

FCS analyzes the intensity fluctuation of fluorescence caused by minute deviations from thermal equilibrium. Fluctuations in the fluorescence signal are quantified by temporally autocorrelating the recorded intensity signal [18-21] (Review: [22]). The fluorescence intensity fluctuation can be analyzed using a fluorescence intensity autocorrelation function (ACF) which is calculated by [19, 23]

$$G(\tau) = \frac{\langle F(t)F(t+\tau)\rangle}{\langle F(t)\rangle^2} = 1 + \frac{\langle \delta F(t)\delta F(t+\tau)\rangle}{\langle F(t)\rangle^2} \tag{1}$$

The brackets describe a time average, F is the fluorescence signal as a function of time, and τ is the correlation time. δF is the fluorescence fluctuations around the mean value. The Brownian motion of particles in a three-dimensional Gaussian volume can be described by the correlation function with [24].

$$G(\tau) = 1 + \frac{1}{N}\left(\frac{1}{1+\frac{4D\tau}{\omega^2}}\right)\left(\frac{1}{1+\frac{4D\tau}{z^2}}\right)^{1/2} \tag{2}$$

N is the number of particles in the confocal volume, D is the diffusion coefficient, ω and z is the radius and axial radii of the laser beam. Diffusion time, τ_D is defined by:

$$\tau_D = \frac{\omega^2}{4D} \tag{3}$$

Therefore, equation (3) can be substituted into equation (2) and get:

$$G(\tau) = 1 + \frac{1}{N}\left(\frac{1}{1+\frac{\tau}{\tau_D}}\right)\left(\frac{1}{1+\left(\frac{\omega}{z}\right)^2\frac{\tau}{\tau_D}}\right)^{1/2} \tag{4}$$

When there are more than two kinds of species in the confocal volume, the intensity autocorrelation function can be analyzed by the following equation [23].

$$G(\tau) = 1 + \frac{\sum_{j=1}^{n} Q_j^2 N_j \left(1+\frac{\tau}{\tau_{D_j}}\right)^{-1}\left(1+\left(\frac{\omega}{z}\right)^2\frac{\tau}{\tau_{D_j}}\right)^{-1/2}}{\left(\sum_{j=1}^{n} Q_j N_j\right)} \tag{5}$$

$$\tau_{D_j} = \frac{\omega^2}{4D_j} \tag{5a}$$

$$Q_j = \sigma_j \eta_j g_j \tag{5b}$$

τ_{D_j} is diffusion time of species j, N_j is the average number of molecules of species j in the confocal volume, D_j is the diffusion coefficient of species j, Q_j is the fluorescence yield, σ_j is the absorption cross section, η_j is the fluorescence quantum yield, and g_j is the fluorescence detection efficiency of species j with the setup. The program Igor Pro 4.0 (Wavemetrics, Lake Oswego, OR ,USA) was used for the fitting of the autocorrelation function to experimental data. [25].

2.4 FCS Experiment

Stock V4-TMR peptide in DMSO (2mM) was diluted with PBS (PH=7.4) to 100 or 200nM. LPS were dissolved in PBS to different concentrations (50, 100, 200, 500, 1000, 2000, and 10000 nM). The mixture of peptide and different concentrations of LPS were incubated for over 4 hours to reach the equilibrium. The dissociation constant *Kd* can be calculated by the following equation [26]:

$$y = \frac{PL^*}{Pt} = \frac{(Lt^* + Pt + Kd) - \left((Lt^* + Pt + Kd)^2 - 4PtLt^*\right)^{1/2}}{2Pt} \tag{6}$$

*PL** is the concentration of bound peptide at equilibrium, *Pt* is the concentration of total concentration of V4-TMR peptide, *Lt** is the total concentration of LPS, and *y* is the fraction of bound peptide.

3.0 RESULTS AND DISCUSSION

The confocal volume was determined to be 0.6 fl by calibration with a solution of 1nM rhodamine 6G. From the diffusion time of rhodamine 6G of 52.6±0.7 μs and the diffusion coefficient D of 280 $\mu m^2/s$, the radii ω of 0.24 μm, and z of 0.96 μm were determined.

V4-TMR peptide showed strong quenching in the PBS buffer compared to a pure TMR solution of equal concentration. We compared the correlation curve of 1 nM TMR, and 100 nM V4-TMR in PBS buffer (Figure 1). For 1 nM TMR, experiments showed an average value of 0.438 particles in the confocal volume, a diffusion time of

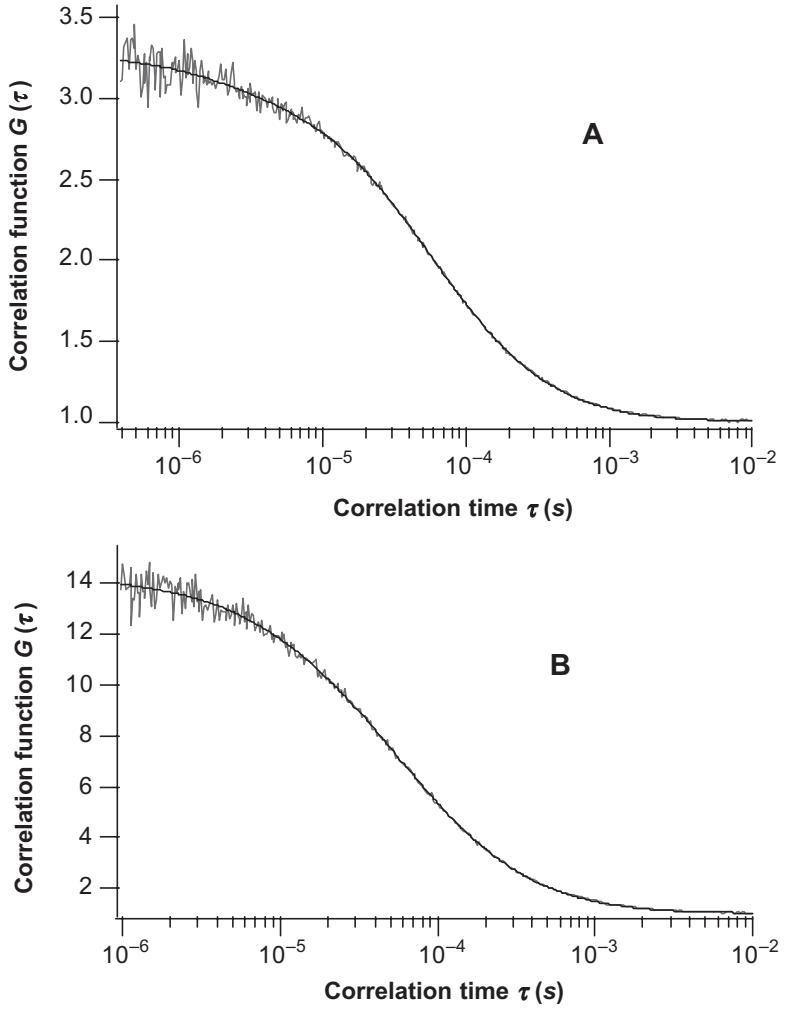

Figure 1 Comparison of correlation curve of TMR and V4-TMR peptide. (a) Correlation function of 1nM TMR. N=0.438, τ_D = 57.0 μs. (b) Correlation function of 100nM V4-TMR peptide. N=0.075, τ_D = 57.8 μs.

57.1±0.1 μs, and an average intensity per particle of 58.7 kHz. For 100 nM V4-TMR peptide, there were only 0.075 particles in the same confocal volume, the diffusion time was 58.4±0.6 μs, and the intensity per particle was 60.4 kHz. Since the characteristic diffusion time and the counts per particle per second are the same in both cases, we suggest that V4-TMR is completely quenched in aqueous solutions, and the fluorescence measured is exclusively attributable to free TMR molecules. Comparing the numbers of particles seen in the two solutions (0.438 for 1 nM TMR, and 0.075 for 100 nM V4-TMR), the proposed impurity of TMR would be 0.17%, which is well within the limits of the manufacturer.

When LPS or lipid A was added to the V4-TMR solution, the fluorescence intensity increased, the number of fluorescent particle increased, and a longer diffusion time was observed. Therefore, we used in all FCS experiments a two species model for data fitting, where one species represents the TMR impurities, and the other species the bound V4-TMR/LPS or V4-TMR/lipid A complexes. Non-bound V4-TMR could not be seen. The intensity per particle of the mixture of V4-TMR with LPS and mixture of V4-TMR with lipid A were determined to be 103, and 109 kHz/molecule respectively, which are much higher than that of the peptide alone. The diffusion times for the V4-TMR/LPS or V4-TMR/lipid A complexes are both on the order of 1 to 2 ms. The diffusion coefficient of bound V4-TMR peptide can thus be calculated to 11.3 $\mu m^2/s$.

Electrostatic and hydrophobic interactions are predominant forces driving the binding between antimicrobial peptides and membranes. Compared to phosphatidylcholine (PC, lipids found for instance in cytoplasmic membranes) a zwitterionic lipid, the binding interaction between peptide and LPS or lipid A which are both negatively charged is much stronger. Maximum binding of V4-TMR to LPS was reached at a concentration of 10 μM of LPS. At the same concentration of lipid A and PC, the binding was reduced by 25 and 90 %, respectively (Table 1). The fact that more peptides bind to the negatively charged lipids shows that electrostatic interaction plays an important role in this process. When peptides bind to the LPS or lipid A, the intensity of fluorescence emitted from the confocal volume increased considerably, and the particles in the confocal volume increased as well (Figure 4 and Table 1). This rise in intensity and increase in observed numbers of particles can be explained by

Table 1 Comparison of interaction of V4-TMR peptide with different lipids.

	Intensity of fluorescence	Particle detected	Intensity per particle	Fraction of bound peptide
Peptide	4505	0.0723	62 309.82	0.053
Peptide and LPS	39 460	0.382	103 298.4	0.901
Peptide and lipid A	12 129	0.111	109 270.3	0.660
Peptide and PC	5337	0.084	63 535.71	0.081

two effects: i) The interaction of V4-TMR and lipids leads to a disaggregation of V4-TMR clusters which previously exist due to the strong hydrophobicity of the peptide, and in which, TMR is strongly quenched. The disaggregation thus leads to an increase in fluorescence as well as an apparent increase in particles observed. ii) TMR comes into a different local environment upon binding (local pH, polarity) leading to an increase in its fluorescence yield. This is comparable to the increase of TMR fluorescence which can be observed upon dissolution in DMSO compared to water (data not shown).

An LPS-concentration dependent experiment was performed to explore the dissociation constant of interaction of V4-TMR with LPS. The dependence of correlation function on the concentration of LPS is shown in Figure 2. With increasing LPS concentration, the fluorescence intensity increased, and the amplitude of the correlation function decreased, which indicates that the number of particles in the confocal volume increased. At the same time, the shape of correlation curve changed with the second species becoming more and more important. Figure 3 depicts the normalized correlation function and shows how the correlation function broadened with increasing binding of V4-TMR to LPS. The detailed fraction of bound peptide in the mixture is shown in Figure 4. The fraction of bound peptide increases with increasing concentrations of LPS. At an LPS concentration of 500 nM, full binding was established. The data is fitted by equation (6), and a dissociation constant of $Kd = (3.34 \pm 0.47) \times 10^{-7}$ M is obtained.

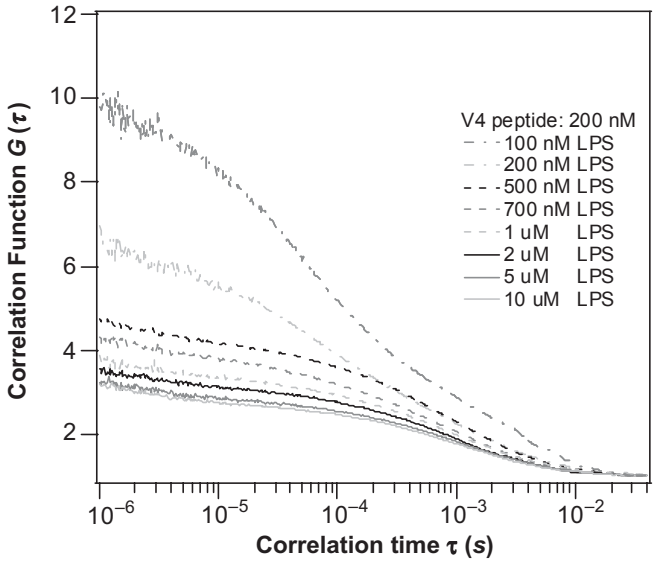

Figure 2 Correlation function with different concentrations of LPS. With the increasing concentration of LPS, the amplitude of the correlation function decreased, and the fraction of bound peptide increased.

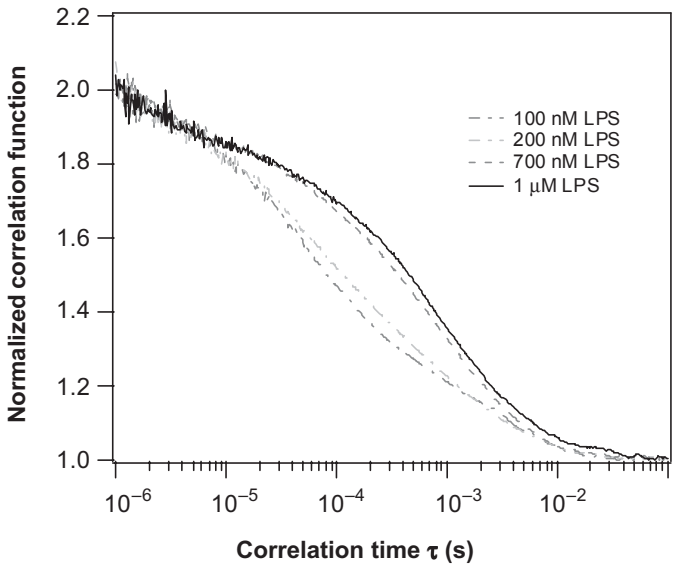

Figure 3 Normalized correlation function with different concentration of LPS. With the increasing concentration of LPS, the average diffusion time increased.

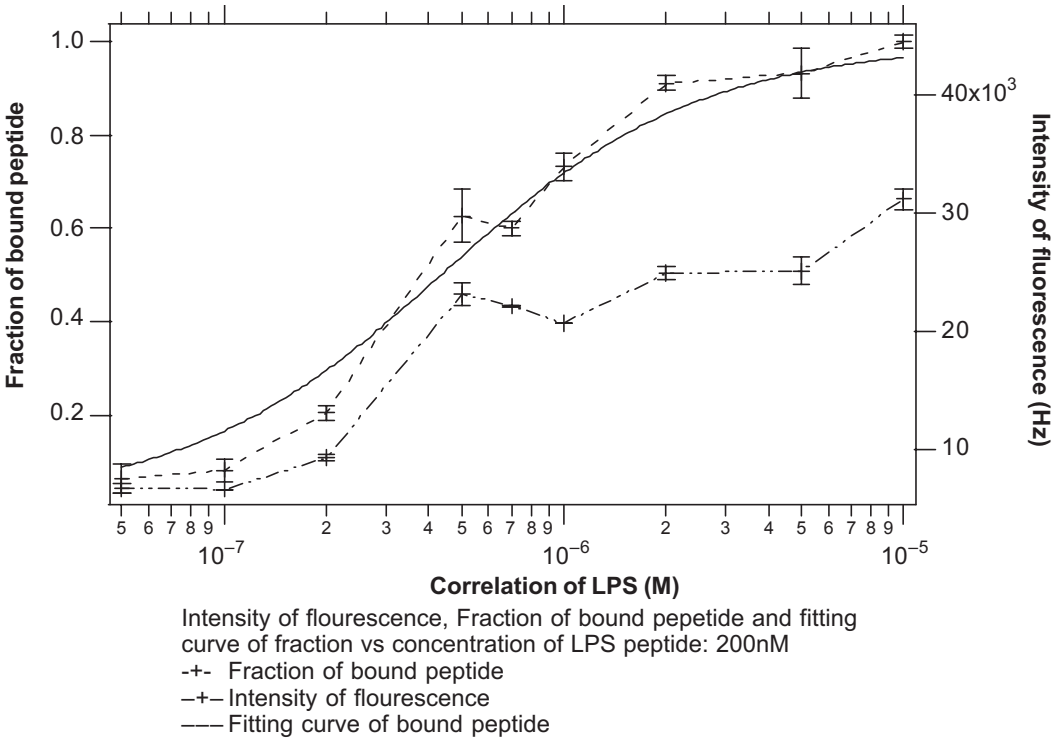

Figure 4 Intensity of fluorescence of sample and fraction of bound peptide both increase with the increasing concentration of LPS.

4.0 CONCLUSION

The experiments demonstrate that the artificial V4 peptide can bind LPS and lipid A efficiently and the interaction can be studied by FCS. V4-TMR shows high selectivity in binding for different lipids. The high positive charge makes the peptide favor binding to negatively charged lipids such as LPS and lipid A, which provide good selectivity for bacterial membranes and cytoplasmic membranes. The high affinity for LPS (Kd = (3.34±0.47)×10^{-7} M) makes this designed peptide a promising candidate for further investigation of antimicrobial activity. This study also suggests that FCS as a sensitive biophysical tool is suitable to study the interaction of antimicrobial peptides and lipids.

ACKNOWLEDGEMENTS

We gratefully acknowledge the support of the NUS for funding and the help of Hwang Lingchin, and Li Peng.

REFERENCES

[1] Barra, D., and M. Simmaco. Amphibian Skin: a Promising Resource for Antimicrobial Peptides. *Trends Biotechnol.* 13: 205-209.

[2] Lehrer, R., and A. K. Lichtenstein. Defensins: Antimicrobial and Cytotoxic Peptides of Mammalian Cells. *Annu. Rev. Immunol*. 11: 105-128.

[3] Mitsuhara, I. 2001. In Vitro Growth Inhibition of Human Intestinal Bacteria by Sarcotoxin IA, an Insect Bactericidal Peptide. *Biotechnol. Lett.* 23: 569-573.

[4] Zasloff, M. 1987. Magainins, a Class of Antimicrobial Peptides from Xenopus skin: Isolation, Characterization of Two Active Forms, and Partial cDNA Sequence of a Precursor. *Proc. Natl. Acad. Sci.* USA 84: 5449-5453.

[5] Shai Y. 1999. Mechanism of the Binding, Insertion and Destabilization of Phospholipid Bilayer Membranes by α-helical Antimicrobial and Cell Non-selectively Membrane-lytic Peptides. *Biochim. Biophys. Acta* 1462: 55-70.

[6] Sitaram, N., and R. Nagaraj. 1999. Interaction of Antimicrobial Peptides with Biological and Model Membranes: Structural and Charge Requirements for Activity. *Biochim. Biophys. Acta* 1462: 29-54.

[7] Heller, W. T., A. J. Waring, and H. W. Huang. 1998. Multiple States of β-sheet Peptide Protegrin in Lipid Bilayers. *Biochemistry.* 37: 17331-17338.

[8] Steiner, H., and D. Hultmark. 1981. Sequence and Specificity of Two Antibacterial Proteins Involved in Insect Immunity. *Nature*. 292: 246-268.

[9] Tossi, A., L. Sandri, and A. Giangaspero. 2000. Amphipathic, α-helical Antimicrobial Peptides. *Biopolymers* (Peptide Science). 55: 4-30.

[10] Selsted, M. E., and S. S. Harwig, 1985. Primary Structure of Three Human Neutrophil Defensins. *J. Clin. Invest*. 76, 1436-1439.

[11] Sokolov, Y., T. Mirzabekov, D. K. Martin, and R. I. Lehrer. 1999. Membrane Channel Formation by Antimicrobial Protegrins. *Biochim. Biophys. Acta* 1420: 23-29.

[12] Oren, Z., and Y. Shai. 1998. Mode of Action of Linear Amphipathic α-helical Antimicrobial Peitdes. *Biopolymers* (Peptide Science). 47: 451-463.

[13] Gazit, E., A. Boman, and Y. Shai. 1995. Interaction of the Mammalian Antibacterial Peptide Cecropin P1 with Phospholipid-vesicles. *Biochemistry*. 34: 11479-11488.

[14] Pouny, Y., and Y. Shai. 1992. Interaction of Antimicrobial Dermaseptin and its Fluorescently Labeled Analogs with Phospholipid-membranes. *Biochemistry*. 31: 12416-12423.

[15] Frecer, V., B. Ho, and J. L. Ding. 2000. Interpretation of Biological Activity Data of Bacterial Endotoxins by Simple Molecular Models of Mechanism of Action. *Eur. J. Biochem.* 267: 837-852 FEBS.

[16] Blondelle, S. E., K. Lohner, and M. Aguilar. 1999. Lipid-induced Conformation and Lipid-binding Properties of Cytolytic and Antimicrobial Peptides: Determination and Biological Specificity. *Biochim. Biophys. Acta* 1462, 89-108.

[17] Holak, T. A., and A. Engstrom. 1988. The Solution Conformation of the Antibacterial Peptide Cecropin-A: a Nuclear Magnetic-resonance and Dynamical Simulated Annealing Study. *Biochemistry.* 27: 7620-7629.

[18] Ehrenberg, M., and R. Rigler. 1974. Rotational Brownian Motion and Fluorescence Intensity Fluctuations. *Chem. Phys.* 4: 390- 401.

[19] Elson, E. L., and D. Magde. 1974. Fluorescence Correlation Spectroscopy. I. Conceptual Basis and Theory. *Biopolym.* 13: 1-27.

[20] Koppel, D. E. 1974. Statistical Accuracy in Fluorescence Correlation Spectroscopy. *Phys. Rev. A.* A10: 1938-1945.

[21] Widergren, J., and R. Rigler. 1998. Fluorescence Correlation Spectroscopy as a Tool to Investigate Chemical Reactions in Solutions and on Cell Surfaces. *Cellular and molecular biology.* 44(5): 857-879.

[22] Krichevsky, O. 2002. Fluorescence Correlation Spectroscopy: the Technique and Its Applications. *Reports on progress in physics.* 65(2): 251-297.

[23] Thompson, N. L. 1991. In Topics in Fluorescence Spectroscopy (Lakowicz, J. R., Ed.) New York: Plenum Press. 337-378.

[24] Aragon, S. R., and R. Pecora. 1976. Fluorescence Correlation Spectroscopy as a Probe of Molecular Dynamics. *J. Chem. Phys.* 64: 1791-1803.

[25] Meseth, U., and T. Wohland. 1999. Resolution of Fluorescence Correlation Spectroscopy. *Biophys. J.* 76: 1619-1631.

[26] Wohland, T., and K. Friedrich. 1999. Study of Ligand-Receptor Interactions by Fluorescence Correlation Spectroscopy with Different Fluorophores: Evidence That the Homopentameric 5-Hydroxytryptamine Type 3_{As} Receptor Binds Only One Ligand. *Biochemistry.* 38(27): 8671-8681.